Comparison of Spacecraft Charging Environments at the Earth, Jupiter, and Saturn

H. B. Garrett, R. Frederickson, and A. Hoffman

Jet Propulsion Laboratory, California Institute of Technology

Studies of the Earth with the ATS-5, ATS-6, and SCATHA spacecraft led to the development of several simple tools for predicting the potentials to be expected on a spacecraft in the space environment. These tools have been used to estimate the expected levels of worst case charging at Jupiter and Saturn for, respectively, the Galileo and Cassini missions. The results of those studies impacted the design and construction of both missions. This paper reviews those results and puts them in the context of the design issues addressed by each mission. In the case of Galileo, spacecraft to space potentials of ~1000 V were predicted. As such levels could produce possible discharges and could effect low-energy plasma measurements, several steps were taken in the design and assembly of the Galileo spacecraft and its surfaces to ameliorate these effects. In particular, the outer surface of Galileo was held to rigid conductivity requirements. Even so, Galileo was not entirely conducting and grounded, necessitating appropriate waivers in some cases. After 14 orbits, however, no adverse effects due to surface charging have been reported. The saturnian environment (as measured by the Voyager spacecraft), in contrast to Jupiter, is shown here to result in spacecraft potentials to space of ~100 V--levels typically well below those of concern to designers, though of some concern to the low-energy plasma experimenters. Cassini was designed with consideration to spacecraft charging issues. The overall surface of the Cassini spacecraft, as in the case of Galileo, was not entirely conducting and grounded. Here it is shown that only in the most extreme (and unlikely) conditions is it expected that Cassini will ever experience any effects of surface charging at Saturn. Those conditions are presented and the likely consequences briefly discussed.

INTRODUCTION

Surface charging is not just a concern for spacecraft in geosynchronous orbit (DeForest and McIlwain, 1971), but also to a varying degree in other regions of the Earth's magnetosphere and throughout the solar system. In particular, high levels of charging (greater than a few hundred volts) are expected in the Earth's auroral zones at high latitudes (Gussenhoven, 1985) and at Jupiter (Divine and Garrett, 1983). Here a simple software tool for estimating surface potentials developed for the Earth's environment is extended to predict surface potentials at Jupiter and Saturn. The results of the tool have been used by missions such as Galileo and Cassini in determining the level and hence design requirements for surface potential mitigation for these missions. Following a brief comparison of the Earth's, Jupiter's, and Saturn's environments, the basic assumptions of the tool will be described and estimated surface potentials for each of these environments presented. The results for Earth and, at least preliminarily, Jupiter and Saturn are consistent with observations demonstrating to first order the value of the tool for mission design.

THE ENVIRONMENTS

Table 1 lists the principle characteristics (from a spacecraft charging standpoint) of the terrestrial, jovian, and saturnian environments--for example, the photoelectron flux at 1 AU is ~25 times that at Jupiter (~5 AU) and ~100 times that of Saturn (~10 AU). More to the point, however, Jupiter and Saturn are roughly 10 times the size of the Earth while their magnetic moments are 10^5 and 10^3 larger. As the magnetic field at the equator is proportional to the magnetic moment divided by the cube of the radial distance, the terrestrial and saturnian magnetospheres roughly scale similarly. The jovian magnetic field, however, scales roughly 100 times larger--indeed, Jupiter's magnetospheric tail has been observed as far downstream as Saturn!

Another aspect of the environment illustrated by Table 1 is the rotation rate. Both Jupiter and Saturn spin over twice as fast as the Earth---~10 hours versus 24 hours. Given their strong magnetic fields, this means that the cold plasma trapped in these magnetospheres is forced to corotate at velocities much higher than the orbital velocity. This is opposite to the Earth, where at low altitudes a spacecraft orbits at ~8 km/s relative to the ionospheric plasma. In

contrast, co-rotation velocities can range from 30-40 km/s near Jupiter and Saturn to over 100 km/s in their outer magnetopsheres. Indeed, even ignoring Saturn's rings and the two giant planets' satellite systems, it is not surprising that these magnetospheres differ greatly from the Earth's. As the magnetosphere is the primary controlling factor for the local plasma environments, the charging environment differs considerably for each of these planets. It is these differences that will be described in the following paragraphs.

Table 1. The Environments

Earth	
-equatorial radius (km)	6.38×10^3
-magnetic moment (G-cm^3)	8.10×10^{25}
-rotation period (hrs)	24.0
-aphelion/perihelion (au)	1.01/0.98
Jupiter	
-equatorial radius (km)	7.14×10^4
-magnetic moment (G-cm^3)	1.59×10^{30}
-rotation period (hrs)	10.0
-aphelion/perihelion (au)	5.45/4.95
Saturn	
-equatorial radius (km)	6.00×10^4
-magnetic moment (G-cm^3)	4.30×10^{28}
-rotation period (hrs)	10.23
-aphelion/perihelion (au)	10.06/9.01

The Earth, despite its small relative size, has one of the most complex and variable magnetospheres in the solar system. As will be shown, it may also have the highest predicted and observed charging levels. In terms of a simple schematic of the Earth's magnetosphere, there are 4 main plasma regions. Starting with the lowest latitude region, the "ionospheric" regime is the extension of the cold ionosphere out along closed field lines to 5 to 6 R_e (typically called the plasmasphere). The plasma varies from a density of ~10^6/cm^3 (O^+ dominated) at 100 km to ~100/cm^3 (H^+) at 4 to 5 R_e. The mean energy varies from a few tenths of an eV to 10-100 eV at the outer edge. At higher latitudes and altitudes lies the auroral regime. This environment is represented by the aurora at low altitudes and the plasmasheet at geosynchronous orbit. The plasma typically consists of an electron/H^+ composition with several 10's of keV mean energy. Superimposed on these two regimes is the Van Allen regime, marked by the trapped radiation belts. These consist primarily of high-energy (E>100 keV) electrons and protons. Although of little direct importance to surface charging, the high-energy electrons are the primary source of internal charging. The final regime, the high-latitude regime, is characterized by low densities (0.1 cm^{-3}) and energies (200 eV) with occasional bursts of high-velocity streams (800 km/s).

The magnetosphere of Jupiter is dominated by three factors: its magnetic field and its tilt (11°), its rapid rotation, and the jovian moon Io at 5 R_j. Io generates a vast torus of neutral gas. The rapid rotation of Jupiter's magnetic field forces the cold plasma associated with this torus to expand by centrifugal force into a giant disc. The magnetic field tilt and rotation rate make this plasma disc wave up and down so that at a given location plasma parameters vary radically over a 10-hour period. Jupiter's environment can be divided into roughly three populations: the cold plasma associated with the Io torus and the plasma disc (0<E<500 eV), the intermediate plasma (500 eV<E<100 keV), and the radiation environment (E>100 keV). The cold plasma is characterized by high densities (~2000 cm^{-3}) and low energies (10-100 eV). The plasma consists of hydrogen, oxygen (singly and doubly ionized), sulfur (singly, doubly, and triply ionized), and sodium (singly ionized) ions. Intermediate-energy electrons (~1 keV) and protons (~30 keV) at Jupiter are assumed to vary exponentially from ~5 cm^{-3} for r < 1 0R_j to 0.001 cm^{-3} beyond 40 R_j. (Divine and Garrett, 1983). Co-rotation velocities vary from ~45 km/s at 4 R_j to ~250 km/s at 20 R_j.

Saturn is marked by a magnificent set of rings that are its most obvious feature and set it apart from all the other planets. Aside from the rings, however, Saturn's magnetosphere resembles Jupiter--a cold inner plasma disk giving way to a lower density, slightly higher energy plasma disk at large distances. Although there is no "Io-equivalent" moon in the inner magnetosphere, there is still a fairly dense cold plasma sheet and, at ~20 R_j, Saturn's huge moon Titan contributes a large cloud of neutral gas in the outer magnetosphere. Unlike Jupiter, Saturn's magnetic field axis is apparently aligned with the spin axis so that the plasma ring around Saturn is relatively stable compared to that of Jupiter. Plasma co-rotation velocities are similar to Jupiter, though maximum velocities tend to peak a little above 100 km/s.

THE MAJOR CURRENT TERMS

Spacecraft designers require simple criteria for determining whether or not surface charging is an issue for a particular mission. As an initial step in the process of developing a mitigation strategy for spacecraft charging, a mathematical model capable of first-order estimates of spacecraft surface-to-space potential for a variety of conditions has been developed (e.g., Tsipouras and Garrett, 1979; Garrett, 1981). The model (or design tool) is based on current balance. Incoming electrons and ions are balanced against photoemission, backscattering, and secondary emission. The program varies the spacecraft-to-space potential until the total current is 0 according to the following equation:

$$I_T(V)=I_E(V)-(I_I(V)+I_{SE}(V)+I_{SI}(V)+I_{BSE}(V)+I_{PH}(V)) \quad (1)$$

Where:

V = surface potential relative to space

I_T= total current to spacecraft surface at V;
= 0 at equilibrium when all the current sources balance
I_E = incident ambient electron current
I_I = incident positive ion current
I_{SE}= secondary emitted electron current due to I_E
I_{SI}= secondary emitted electron current due to I_I
I_{BSE} = backscattered electron current due to I_E
I_{PH} = photoelectron current

The incident electron and ion currents are typically estimated by integrating the appropriate Maxwellian distributions (Eq. 2) to obtain the current as a function of temperature, number density, and potential. The secondary and backscatter surface currents are then obtained by integration using the Maxwellians--the results have been parameterized by fitting them in terms of the temperature, number density, and potential (see Tsipouras and Garrett, 1979; and Garrett, 1981). Aluminum is used in this study as the surface material. The photoelectron current is similarly parameterized in terms of the potential and material.

2) $F_M = N(M/2\pi E_o)^{3/2} e^{-E/E_o}$

Where:

F_M = Maxwell-Boltzmann distribution

N = Number density

E_o = Characteristic energy of plasma

E = plasma energy

Whereas Maxwellian distributions adequately represent many of the plasma environments encountered in space, they are often inadequate for explaining the complex environments at Jupiter and Saturn. Indeed, for co-rotating ion plasmas, a "ram" approximation is often more appropriate:

3) $I_R = \pi R^2 N V_S$

Where:

I_R = "Ram" current

V_S = Spacecraft velocity relative to plasma

R = Radius of spherical spacecraft

The Jovian and Saturnian environments are characterized by a much harsher radiation environment at high energies than the Earth's. As a result, a Maxwellian distribution does not join smoothly onto the high-energy spectra for the protons and electrons. If the latter power law spectra are cut off at an arbitrary low energy, the resulting discontinuity causes difficulties, in particular, in computing the total current density of the electrons to a satellite surface in the jovian environment. To derive a smooth distribution function for the warm electrons and protons, the Kappa distribution function F_κ in cm^{-6}-s^3 (see Vasyliunas, 1968) was employed:

4) $F_\kappa = N(M/2\pi E_o)^{3/2} \kappa^{-3/2} \frac{\Gamma(\kappa+1)}{\Gamma(\kappa-1/2)} \frac{1}{(1+E/\kappa E_o)^{\kappa+1}}$

Where:

F_κ = Kappa distribution

Γ = Gamma function

κ = Kappa factor (constant)

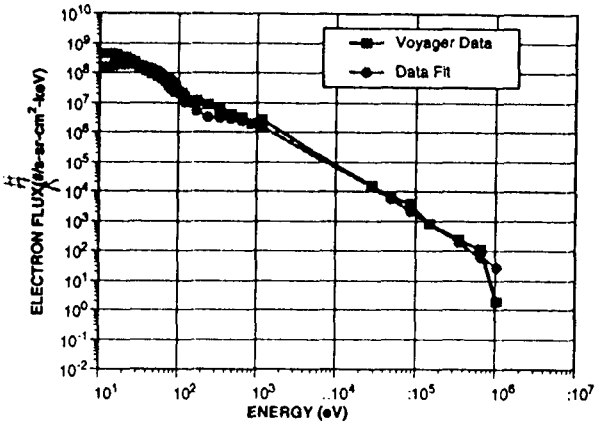

Fig. 1. Maxwellian (below 1 keV) and Kappa (above 1 keV) distribution fits to Voyager 2 inbound electron measurements for Saturn (L=11.59). The potential was estimated to be -480 V in the absence of sunlight and secondary emission for this environment.

As κ goes to infinity, Eq. 2 becomes a Maxwellian distribution. As E goes to infinity, the form of the distribution approaches a power law. A simple fitting procedure was utilized to determine the values for these parameters. First, the omnidirectional high-energy fluxes were computed and converted to values of the distribution function at two energies for electrons (36 and 360 keV) and for protons (0.6 and 6 MeV). The values of the warm electron and proton Maxwellian density and temperature were used to determine values of the distribution function at zero energy. A representative fit for Saturn is presented in Fig. 1. The resulting Kappa distributions were then integrated to give appropriate surface currents as functions of temperature, κ, number density, and potential.

ESTIMATED CHARGING LEVELS--MISSION PLANNING

Given a model of the ambient electron and ion environments in terms of Maxwellian and Kappa distributions and the density and co-rotation velocity of the cold ions, the surface potential for a spacecraft surface can be estimated using the simple spacecraft-to-space thick

sheath model described above. Evans et al. (1989) used this method to calculate the potentials throughout the terrestrial magnetosphere for a small aluminum sphere in the Earth's shadow. Their results are presented in Fig. 2. The potentials in this figure correspond well with actual observations. This figure is intended to be used as a simple mission planning tool for identifying regions with high charging levels--if a spacecraft were to pass through a region of high charge, then appropriate mitigation methods should be considered in the design.

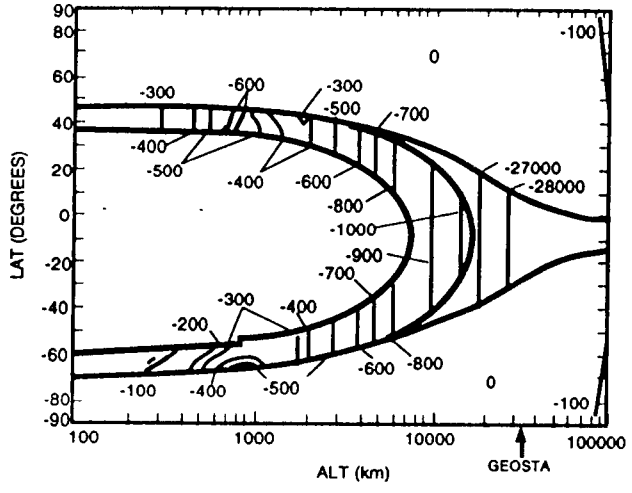

Fig. 2 Surface potential contours (in the absence of sunlight) in volts as a function of altitude and latitude for the Earth (Evans et al., 1989).

As in the case of the Earth, spacecraft designers are concerned with surface charging at Jupiter and Saturn. Unlike the Earth, however, over a large portion of the jovian and saturnian magnetospheres warm energetic electron fluxes are the dominate current source, balancing principally with the photoelectrons. As mentioned earlier, it has proven necessary to represent the 1 to 100 keV electron energy range by a kappa distribution rather than by a combination of Maxwellian terms. In Fig. 3, from Divine and Garrett (1983), the spacecraft-to-space potentials for the jovian magnetosphere have been estimated using the design tool. The potential contours represent the spacecraft-to-space potentials that would be seen for a conducting sphere in the sunlight (note: the charging model does not accurately predict positive potentials above 10 V, as these are not likely in nature). These observations are in good agreement with those reported for Voyager by Scudder et al. (1981) and McNutt (1980). This latter paper implied that on one occasion a potential of -130 V might have been observed. The former paper reported potentials of a few tens of volts positive and tens of volts negative in the torus.

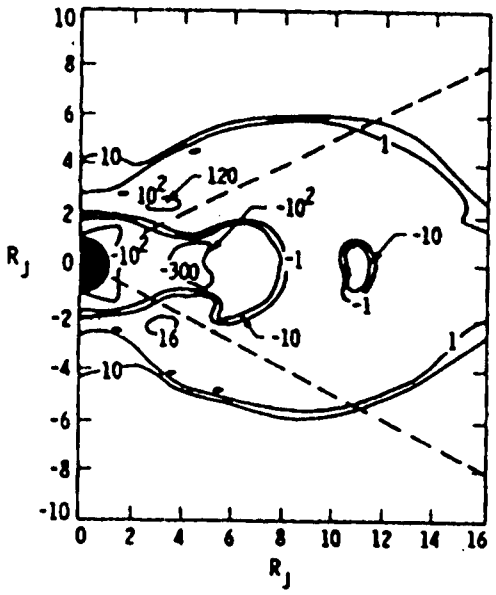

Fig. 3. Spacecraft-to-space potential contours in volts for the thick sheath approximation in the 110°W meridian at Jupiter (Divine and Garrett, 1983). The horizontal axis represents distance along the rotational equator. Photoelectron and secondary electron currents are included. The dashed lines bracket the region of applicability (observations).

It should not be assumed from Fig. 3 that spacecraft charging is not a problem in the jovian environment. Under fairly restrictive conditions, secondary emissions can be suppressed over a small surface (e.g., Fig. 4). If that surface is electrically isolated from the vehicle and in the shade so that the photoelectron flux is zero, significant charging can occur, as evidenced in Fig. 5. In support of such predictions, the Voyagers may have observed tens of kV surface potentials at Jupiter (Khurana et al., 1987). Fortunately, the Voyager and Galileo spacecraft were designed to be conductive over most of their surfaces and approached the ideal of a conducting sphere.

The charging environment at Saturn resembles that at Jupiter. To date, however, a comprehensive plasma model such as developed for Jupiter has not been completed. Instead, a set of 16 electron and ion spectra covering the L-shell range from ~4 to ~21 have been reconstructed from the Voyager 1 and 2 flybys (Krimigis et al., 1983; Richardson and Sitler, 1990; Maurice et al., 1996) for the purpose of estimating the expected potentials. A representative electron spectrum is presented in Fig 1. Each set of electron spectra were fit by a Maxwellian at low energies (~10 to 1000 eV) and a Kappa distribution from 1 keV to 100 keV. The cold plasma populations (hydrogen and oxygen ions) were fit by

either a Maxwellian or co-rotation velocity. The proton population above 1 keV was fit by a Kappa distribution.

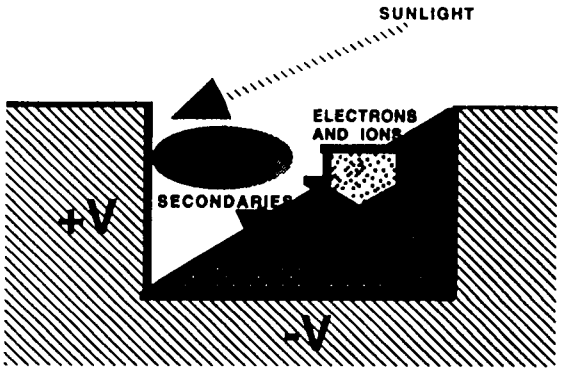

Fig. 4. Schematic illustrating one way the secondary emission of electrons might be suppressed over a surface.

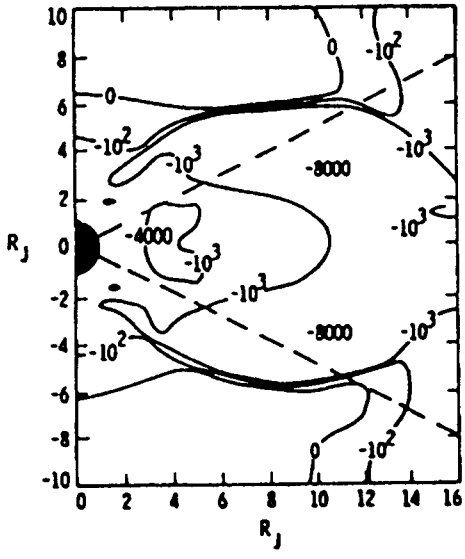

Fig. 5. Spacecraft-to-space potential contours for the thick sheath approximation (Divine and Garrett, 1983) as in Fig. 3. No photoelectron or secondary currents are included.

Fig. 6 gives the potentials calculated by the tool for sunlit and shadowed conditions. Two cases are shown for the cold ions--thick (sheath) and ram. The thick sheath case, as described in Garrett (1981), assumes the cold ions are best described by a Maxwellian plasma. The ram case assumes the cold ion current is best represented by a co-rotating flow (see Eq. 3). In reality, the actual current lies between these two limits but closer to the thick sheath limit. Fig. 13 basically shows that even though the photoelectron flux is very low at Saturn (100 times lower than at the Earth), the plasma charging environment is relatively benign. Surface potentials might reach a few tens to a hundred volts negative only in the outer magnetosphere.

Again, however, this is not the whole story. In Fig. 7, the potentials were estimated assuming that the spacecraft was in shadow and that either the cold ions (as when they are shadowed on one side of the spacecraft) or the secondary electrons were suppressed. For those cases (and either ram or thick sheath), the potential can reach several hundred volts negative between 8 and 18 L. Although Cassini was designed to be conductive on the outside, this was not entirely successful. There may be some areas on Cassini that can charge. However, as all areas where charging or arcing might be a concern were covered with conducting materials before launch, charging will not likely impact the mission.

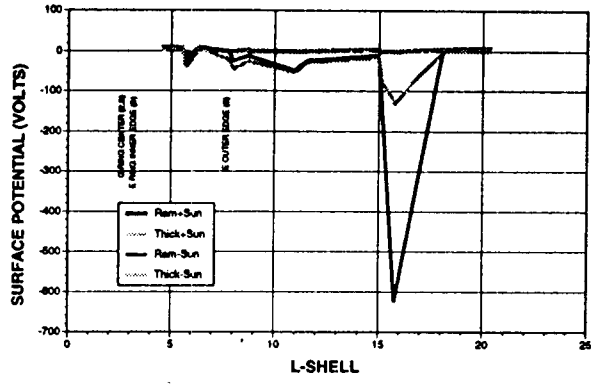

Fig. 6. Spacecraft-to-space potentials in sunlight and darkness for Saturn as a function of L-shell. For one set, the ion current is assumed proportional to its thermal (thick sheath) value. In the other, it is set equal to the ram current (Eq. 3).

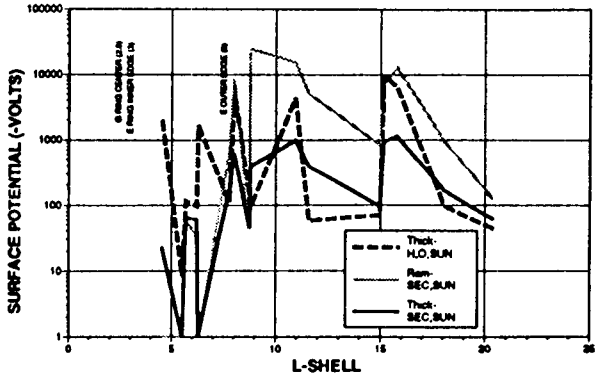

Fig. 7. Spacecraft-to-space potentials (negative) in darkness for Saturn as a function of L-shell. For two of the estimates, the secondary current has been set equal to 0. As in Fig 5, for one set, the co-rotating ion current is assumed proportional to its thermal (thick sheath) value while in the other, it is set equal to the ram current (Eq. 3). For the third set, the co-rotating ions have been set equal to 0.

CONCLUSIONS

To conclude, a simple design tool based on current balance and descriptions of the Earth's, Jupiter's, and Saturn's plasma environments in terms of Maxwellian and Kappa distributions and, for the cold ions, the corotating velocity have been combined to estimate the spacecraft-to-space potentials for missions to these planets. The results of this tool for a spherical spacecraft with aluminum surfaces are presented in Table 2 for several different situations. Based on this table, the Earth clearly represents the worst threat to spacecraft. Negative potentials as high as 28,000 V are predicted near geosynchronous orbit in eclipse and, indeed, potentials in excess of -20,000 V have apparently been observed. At Jupiter, potentials are more moderate. Large potentials are only observed if secondary emissions can be suppressed--unlikely but possible for some surface configurations. Conditions at Saturn are similar to those at Jupiter, though somewhat lower. Even so, spacecraft surface charging is still a concern, albeit low-level threat for spacecraft survivability at these planets. Indeed, as potentials of even a few 10's of volts can seriously affect low-energy plasma measurements, spacecraft charging must be considered for most missions to these giant planets.

Table 2. Estimated charging levels at the Earth, Jupiter, and Saturn for a simple charging design tool.

	V_e(km/s)	Potential(V) Sun	No Sun/Sec
Earth			
-ionosphere	8	-0.7	-4.4
-plasmasphere	3.7	-1.6	-3.8
-auroral zone	8	-0.7	-500
-geosynchronous	3	2.0	-28,000
Jupiter			
-cold torus	44	-.59	-1.2
-hot torus	100	-60	-70
-plasma sheet	150	-94	-130
-outer mag-sph	250	9.5	-2500
Saturn			
-inner plasma sheet	100	~5	-30
-outer plasma sheet	100	~5	-500
-hot outer mag-sph	100	~5	-500

ACKNOWLEDGMENTS

The research in this paper was carried out by the Jet Propulsion Laboratory, California Institute of Technology, under contract with the National Aeronautics and Space Administration.

REFERENCES

DeForest, S.E., and C.E. McIlwain, "Plasma Clouds in the Magnetosphere," *J. Geophys. Res.*, Vol. 76, 1971, pp. 3587.

Divine, T.N., and H.B. Garrett, "Charged particle distributions in Jupiter's magnetosphere," *J. Geophys. Res.*, Vol. 88, Sept. 9, 1983, pp. 6889-6903.

Evans, R., H.B. Garrett, S. Gabriel, and A.C. Whittlesey, "A Preliminary Spacecraft Charging Map for the Near Earth Environment," *Spacecraft Charging Technology Conference*, Naval Postgraduate School, 1989.

Garrett, H.B., "The Charging of Spacecraft Surfaces," *Rev. Geophys.*, Vol. 19, 1981, pp. 577-616.

Gussenhoven, M.S., "High-Level Spacecraft Charging in the Low Altitude Polar Environment," *J. Geophys. Res.*, Vol. 90, 1985, p. 11009.

Khurana, K.K., M.G. Kivelson, T.P. Armstrong, and R.J. Walker, "Voids in Jovian Magnetosphere Revisited: Evidence of Spacecraft Charging," *J. Geophys. Res.*, Vol. 92, No. A12, 1987, pp. 13,399-13,408.

Krimigis, S. M., J. F. Carbary, et. al., "General characteristics of hot plasma and energetic particles in the Saturnian magnetosphere: Results from the Voyager spacecraft," J. Geophys. Res., Vol. 88, pp. 8871-8892 (1983).

Maurice, S., E. C. Sitler, Jr., et. al., "Comprehensive analysis of electron observations at Saturn: Voyager 1 and 2," J. Geophys. Res., Vol. 101, pp. 15,211-15,232 (1996).

McNutt, R. L., Jr., "The dynamics of the low energy plasma in the Jovian magnetosphere," Ph.D. Thesis, Massachussetts Institute of Technologly, Cambridge, MA, (1980).

Richardson, J. D., and E. C. Sitler, Jr., "A plasma density model for Saturn based on Voyager observations," J. Geophys. Res., Vol. 95, pp. 12,019-12,031 (1990).

Scudder, J. D., E. C. Sittler, Jr., and H. S. Bridge, "A Survey of the Plasma Electron Environment of Jupiter: A View From Voyager," J. Geophys Res., Vol. 86, pp. 8157-8179 (1981).

Tsipouras, P., and H. B. Garrett, "Spacecraft Charging Model-Two Maxwellian Approximation," AFGL-TR-79-0153, 1979.

Vasyliunas, V. M., "A Survey of Low-energy Electrons in the Evening Sector of the Magnetosphere with OGO 1 and OGO 3," J. Geophys. Res. , Vol. 73 , pp. 2839 (1968).